3D Imaging of a Manmade Target with Weak Scattering Centres by Means of UWB-Radar

Rahmi Salman, Ingolf Willms
Fachgebiet Nachrichtentechnische Systeme (NTS)
Universität Duisburg-Essen
Duisburg, Germany
E-Mail: salman@nts.uni-due.de

Takuya Sakamoto, Toru Sato
Graduate School of Informatics
Kyoto University
Yoshida Honmachi, Sakyo-ku
Kyoto 606-8501, Japan

Alexander Yarovoy
Microwave Sensing, Signals and Systems
Delft University of Technology
Delft, the Netherlands

***Abstract*—In this paper a 3D bi-static, fully polarimetric Ultra-Wideband (UWB) imaging system which satisfies super-resolution conditions is presented. The objective is to inspect a target with weak scattering centres and to prove the performance of recent imaging methods under these conditions. This issue is handicapped further by spanning a suboptimal synthetic array, i.e. the main beam of the antennas is not aligned with the orientation of the weak scatterers. An opened laptop with a knife fixed at the back of the display is used as the target for an experimental validation. The radar cross section of the keyboard in this position can be assumed to be very small which reveals very weak multibounce scattering mechanisms. The evaluation of the imaging is performed by the real-time capable revised range point migration (RRPM) and the conventional Kirchhoff migration. The experimental validation is carried out with a pair of two tapered slot line Vivaldi antennas both integrated in a conical shaped teflon rod and an M-sequence Radar device with 100% fractional bandwidth at a carrier of 9 GHz.**

Keywords— Kirchhoff Migration; Microwave Imaging; UWB Imaging; UWB Radar; Revised RPM; Weak Scattering Centres.

I. INTRODUCTION

Interpreting radar images of complex targets has always been a challenging issue, especially for narrow-band systems. Since range resolution and therewith multipath immunity is proportional to the absolute bandwidth, immense improvements could be achieved with extensive research on UWB-Radar technology [1]. By now, super-resolution imaging of complex objects with contour variation of only a couple of centimetres can be resolved to a satisfying degree. Additionally, UWB-Radar is not restricted by dense smoke, dust and other particles compared to conventional sensors, e.g. infrared, ultrasound or optics. Subject to the presence of low frequencies UWB even operates in- or through-wall. With regard to these features UWB technology has a superior potential concerning emergency scenarios. Moreover, due to the huge bandwidth the power spectral density is extremely low which enables coexistence with other narrowband radio systems. However, many super-resolution methods deal with an ideal synthetic aperture where the antenna alignment is perfectly matched to the scattering centres of the target under test. This strategy ensures strong echoes due to high radar cross section values. But, in case that the scattering centres are covered just by the antenna side lobes (which may easily be the case especially with narrow main beam antennas) the echoes become weak. In the worst case a detection, classification or imaging may be difficult or even impossible. Other reasons for weak scattering centres are low SNR, low dynamic range of the hardware device and materials with low permittivity.

II. HARDWARE SETUP AND SYSTEM DESIGN

In this paper the challenge of weak scattering centres shall be addressed and discussed. For this purpose an usual 15-inch laptop is scanned by a bi-static antenna configuration on a circular antenna track at different heights. The display is opened at right angle to the keyboard and an additional knife of 35 cm length is fixed at the back of the display. A photograph of the scenario is shown in Fig. 1.

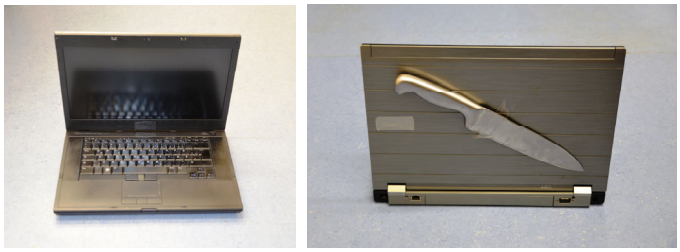

Figure 1. Target under test

The laptop is positioned 90 cm in front of the antennas which are oriented to the laptop. In this setup a circular track is performed at different heights at 0.5 cm interval starting at the bottom of the laptop until its top. Consequently, the antennas have no proper alignment with regard to the keyboard. Additionally, the diffuse multi bounce scattering caused from the keyboard is masked with double bounce contributions from the display to the keyboard and finally to the receiver. The grip of the knife is approximately 3 cm in diameter whereas the blade is just a couple of millimetre thick. For the purpose of illustration a radargram of one measured circular track at half of the height is depicted in Fig. 2.

978-1-4799-0969-8/13/$31.00 ©2013 IEEE

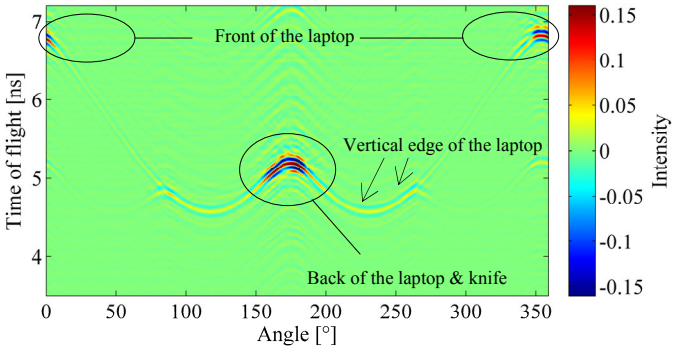

Figure 2. Radargram of the target taken at half of the height

A. Radar Device and Antennas

An UWB Maximum Length Binary Sequence (M-Sequence) Radar system with an operating band of DC–4.5 GHz was used within these investigations. For higher time resolution an additional quadrature modulator was used which operates with a carrier frequency of 9 GHz and doubles the bandwidth. Thus, the operating frequencies occupy the band of 4.5 GHz up to 13.5 GHz with an absolute bandwidth of 9 GHz.

A pair of directive Teflon embedded two tapered slot line Vivaldi antennas on a single substrate [1][2] were used for the investigations. The antennas have a satisfying matching with an s-parameter s11 less than 10dB in the whole range. With an antenna gain of up to 15 dBi and a narrow 3dB beam width of 25° the antenna characteristic satisfies the requirement of short-range super-resolution imaging. However, in certain circumstances the sharp focusing characteristic may also be disadvantageous, e.g. to properly gather spatially distributed energy when a target under test is not in the main lobe of the antennas. This is the case with the keyboard within this scenario.

III. IMAGING ALGORITHM

The concept of microwave imaging by means of electromagnetic waves is based on synthetic aperture Radar (SAR). Instead of using one sensor with a large real aperture, the antenna motion generates a synthetic aperture. Within this track the target interacts with the transmitted UWB pulses and is characterised by diffraction, reflection, and scattering. These effects are determined by the geometry of the objects, the operating frequency, the material composition and the polarisation of the incident wave. Thus, all received pulses have to be processed concerning their spatial and temporal signature subject to the local coordinate of the point of acquisition. Imaging is performed by the real-time capable revised range point migration (RRPM) and the conventional Kirchhoff migration

A. Revised Range Point Migration

Many of the conventional imaging methods for UWB Radars are based on the back-propagation or optimization process [3][4][5][6], which makes the computational burden too large, in particular, for security systems because real-time or sub-real-time operations are necessary for the application. Recently, the RRPM was developed and has been considered promising for this purpose [7]. The method was proposed to quicken the computation for UWB radar imaging, and is based on two principles: the inverse boundary scattering transform (IBST) [8] and weighted averaging to estimate stable derivatives of the target range in terms of the antenna position.

The IBST was originally derived for mono-static radar systems, but can also be applied to bi-static radar systems by modifying the formulation. This method first estimates the peak points of the signal by estimating multiple combinations of (θ_i, h_i, t_i) $(i = 1, 2, \cdots, Q)$ that satisfy the following conditions:

$$\begin{aligned} &\frac{\partial}{\partial t} s(\theta, h, t) = 0 \\ &\left| s(\theta, h, t) \right| > \alpha \max \left| s(\theta, h, t) \right| \end{aligned} \tag{1}$$

where $s(\theta, h, t)$ is a received signal after applying pulse compression for an antenna midpoint at a height h, a rotational angle θ, and delay time t. To prevent noise component from picked, the threshold α is introduced and set to be $\alpha = 10^{-4}$ in this paper. At each antenna position, a tangent plane $\bar{x} - \bar{y}$ is assumed to apply the IBST described below. Note that in this scanning antenna configuration, $\bar{y} = h$ and $\bar{x} = R\theta$, where R is the radius of the scanning cylindrical surface. The number of points picked in the algorithms is set to be $Q = 15 \times 11 \times 360$, which means that 15 peak points are picked at each antenna position.

The IBST for a bi-static configuration with a curved scanning surface is expressed [9] as

$$\begin{aligned} \bar{x} &= \bar{X} - \frac{2D^3 D_{\bar{X}}}{D^2 - d^2 + \sqrt{\left(D^2 - d^2\right)^2 + 4d^2 D^2 D_{\bar{X}}{}^2}} \\ \bar{y} &= \bar{Y} + \frac{D_{\bar{Y}}}{D^3}\left(d^2 (\bar{x} - \bar{X})^2 - D^4\right) \\ \bar{z} &= \bar{Z} + \sqrt{D^2 - d^2 - (\bar{y} - \bar{Y})^2 - \frac{(D^2 - d^2)\left(\bar{x} - \bar{X}\right)^2}{D^2}} \end{aligned} \tag{2}$$

where a bar on the variables means that the coordinate system is transformed from the original coordinate system so that the antenna spacing is in the direction of x, and the x-y plane is tangent to the scanning surface. A point (x, y, z) is the scattering centre on the target surface, X, Y and Z are the x-, y- and z-coordinates of the midpoint of the antenna positions and D is the half length of the propagation path, which is estimated by extracting peaks of the received signals. Dx and Dy are the derivative of the D with respect to x and y. The derivatives Dx and Dy are sensitive to noise and interference, making the IBST difficult to directly apply to complicated scenarios like in this paper. To stabilize the IBST, we developed the RRPM that estimates the derivative for the i-th peak point using weighted averaging of numerous peak points as in

$$D_{\bar{X}i} = \tan\left(\frac{\sum_{j\neq i} w_{i,j} \tan^{-1}\left(\frac{D_i - D_j}{X_i - X_j}\right)}{\sum_{j\neq i} w_{i,j}}\right) \quad (3)$$

$$w_{i,j} = |s_i s_j| \exp\left(-\frac{(X_i - X_j)^2}{\sigma_X{}^2} - \frac{(D_i - D_j)^2}{\sigma_D{}^2}\right) \quad (4)$$

where X_i and D_i are the i-th antenna position and the corresponding range, $w_{i,j}$ is the weighting coefficient that has a large value if $|D_i\text{-}D_j|$ and $|X_i\text{-}X_j|$ are both small. By averaging multiple points as in (3), the estimate of the derivative is statistically stabilized even for noisy data. The derivative with respect to y is also estimated in the same way as Eqs. (3) and (4), giving the derivative $D_{\bar{Y}i}$ for the i-th peak point. We finally obtain the target image by substituting both estimated derivatives of (3) to (2). We set the parameters as σ_X = 1.0 cm and σ_D = 1.0 cm in this paper.

B. *Kirchhoff Migration*

The second imaging algorithm used in this work is Kirchhoff migration (KM). KM is a popular imaging algorithm based on SAR principles which is extensively analysed in the literature [6]. KM has a low computational complexity and is rather simple to adapt to arbitrary scenarios. The concept of KM is a back projection of the radiation characteristic and relies on some form of coherent summation. Thus, a pixel of the Radar image is produced by integrating the phase-shifted Radar data of each antenna position. The mathematical formulation can be expressed as

$$p(x,y) = \frac{1}{N}\sum_{n=1}^{N} h_n\left(\frac{d_{TXn} + d_{RXn}}{c_0}\right) \quad (5)$$

where N is the number of measurements which contribute to a pixel with the (x,y)-coordinate. The n-th measured channel impulse response in time domain is $h_n(t)$, d_{TXn} and d_{RXn} are the distances between $p(x,y)$ and the transmit and receive antenna, respectively. The speed of light is c_0. In case of a bi-static configuration this algorithm summarises the impulse response values along wavefronts which equal ellipses. At positions where objects cause a reflection and therewith increase the values in the impulse response, the ellipses superpose to pixels of high intensity. The image contrast is higher with increasing number of recorded impulse responses at different non-linear positions.

However, the superposition also leads to image artefacts because the ellipses do not only intersect at scattering centres. Hence, this ambiguity of intersection of ellipses decreases the spatial resolution and yields erroneous pixels. Moreover, even in an image area where the ellipses do not intersect the noise floor is increased by the ellipses themselves which reduces the signal to noise and signal to clutter ratio. To some extent and under special circumstances (dense clutter with positions near to objects of interest) these artefacts can make the interpretation of the resulting image difficult or even impossible.

IV. EXPERIMENTALLY VALIDATED RESULTS

A. *RRPM Image*

The RRPM was processed mono-polarized with HH data where the first index indicates the polarization of the transmitter and the second the one of the receiver. The difference of dual- or quad-polarized data was negligibly small and is not considered further. This is because the RRPM uses a threshold to pick discrete points as in Eq. (1), making the image less sensitive to the signal amplitude and polarization characteristics. Actually, the original image obtained by the RRPM is expressed as a cluster of binary pixels. However, within the post processing each pixel is projected to the grid data with a weight of the signal amplitude to indicate the strength of the scattering centre. The extracted image by the RRPM algorithm is shown in Fig. 3.

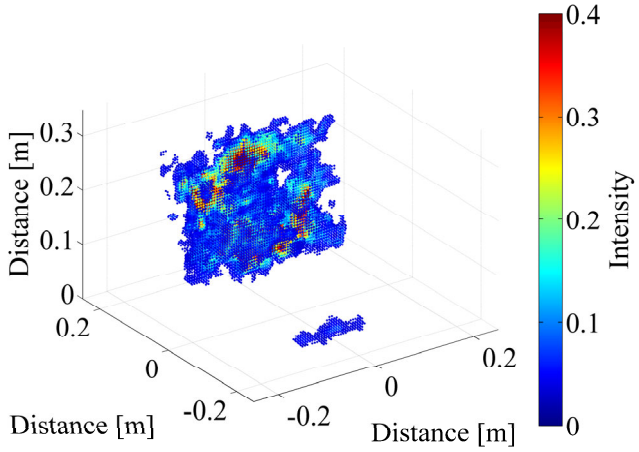

Figure 3. HH image obtained with RRPM

B. *Kirchhoff Images*

The imaging by the KM was applied onto dual-polarized Radar data because it provides supplemental information on parts of the target geometry which are associated with certain elementary scattering patterns. Both co-polarizations are processed, i.e. HH and VV. The visualisation of a 3D image in this 2D document is presented by significant slices positioned in the 3D coordinate system.

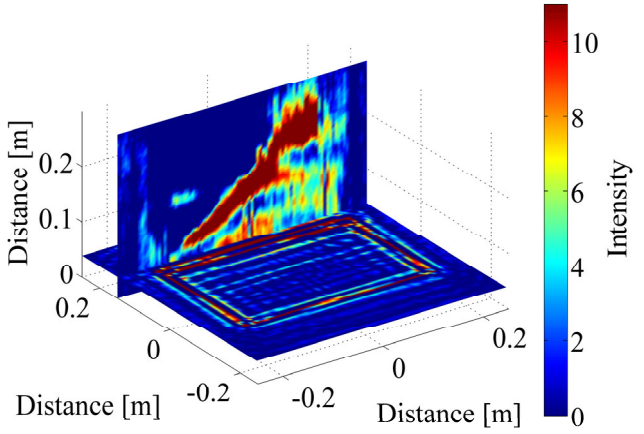

Figure 4. HH image obtained with the KM

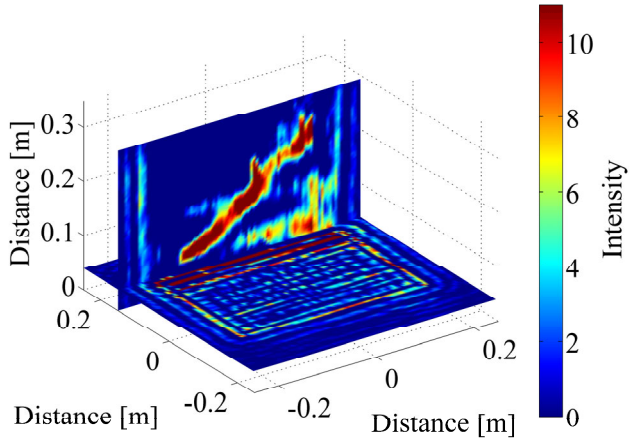

Figure 5. VV image obtained with the KM

V. Discussion and Conclusion

The RRPM image in Fig. 3 provides an image of the display as well as a part of the front edge of the keyboard. The KM images in Fig. 4 and Fig. 5 clearly extract the display, the knife, the keyboard and the right angle of the connection between the display and the keyboard. In terms of polarimetric terminology this connection equals a dihedral which provides strong echoes. Also the edges of the display and of the keyboard are clearly extracted and (depending on the polarization state) emphasized to a different degree. In the HH measurement the edges of the keyboard frame have high values because of horizontal orientation. Both vertical edges of the display (to the right and left) are more visible in VV condition because of same the reason.

The overwhelming advantage of RRPM is its ultra-fast computation which makes it attractive for practical emergency application. However, the image quality is strongly depending on the correct estimation of the wavefronts. This issue faces following main problems:

- A proper alignment of the antennas is indispensable. Especially directive antennas with a narrow beam illuminate just a small area of the target and get rid of the remaining parts.
- Weak scattering centres may reveal wavefronts which cannot be detected due to low SNR or hardware given restrictions (antenna ringing, too low fractional bandwidth) and consequently cannot be imaged by the RRPM.

The weak scattering centres of the keyboard and the antenna misalignment are the reason why the keyboard is not extracted by the RRPM. The KM avoids this issue by coherently summing hundreds of measurement values which are associated with the keyboard. Even if the reflection is very weak, the summation provides a visible imaging or at least an indication which can be interpreted.

The height deviations between the flat display and parts of the knife are in the range of a few mm at the blade and up to 3cm at the grip. This combination causes single bounce from the knife itself, single bounce from the display and higher order bounces from the cavity between knife and display. A superposition of all effects causes serious interference which are hardly resolvable. The KM avoids this again by summarizing a vast amount of scattering signatures of this area which highlights the scattering centres.

The performance concerning image quality and contrast enhancement are resolved more precisely by the KM but at the expense of computation time. Due to the vast computational load the KM is rarely real-time capable. The RRPM is definitely real-time capable but has deficiencies in scenarios with weak scattering centres and strong interfering conditions.

References

[1] R. Zetik, H. Yan, E. Malz, S. Jovanoska, G. Shen, R.S. Thomä, R. Salman, T. Schultze, R. Tobera, I. Willms, L. Reichardt, M. Janson, T. Zwick, W.Wiesbeck, T. Deißler, J. Thielecke. "*Cooperative Localization and Object Recognition*" in UKoLoS Ultra-Wideband Radio Technologies for Communications, Localization and Sensor Applications. R.S. Thomä, R. Knöchel, J. Sachs, I. Willms, T. Zwick (Eds.). InTech Academic Publisher, ISBN: 978-953-307-740-6.

[2] R. Salman, I. Willms, L. Reichardt, T. Zwick, W. Wiesbeck, "On Polarization Diversity Gain in Short Range UWB-Radar Object Imaging", 2012 IEEE International Conference on Ultra-Wideband (ICUWB), Syracuse, USA, Sept. 2012.

[3] D.L. Mensa, D. Heidbreder, G. Wade, "Aperture synthesis by object rotation in coherent imaging," IEEE Trans. Nucl. Sci., vol. NS-27, no. 2, pp. 989-998, Apr. 1980.

[4] D. Liu, J. Krolik, L. Carin, "Electromagnetic target detection in uncertain media: Time-reversal and minimum-variance algorithms," IEEE Trans. Geosci. Remote Sens., vol. 45, no.4, pp. 934-944, Apr. 2007.

[5] A. G. Yarovoy, T. G. Savelyev, P. J. Aubry, P. E. Lys, L. P. Ligthart, "UWB array-based sensor for near-field imaging," IEEE Transactions on Microwave Theory and Techniques, vol. 55, no. 6, part 2, pp. 1288-1295, June 2007.

[6] X. Zhuge, A. G. Yarovoy, T. Savelyev, L. Ligthart, "Modified Kirchhoff migration for UWB MIMO array-based radar imaging" IEEE Transactions on Geoscience and Remote Sensing, vol. 48, no. 6, pp. 2692–2703, 2010.

[7] T. Sakamoto, T. Savelyev, P. Aubry, A. Yarovoy, "Fast Range Point Migration Method for Weapon Detection using Ultra-Wideband Radar," IEEE 9th European Radar Conference, EuRAD, 31.10.-02.11.2012, Amsterdam, The Netherlands.

[8] T. Sakamoto, T. Sato, "A target shape estimation algorithm for pulse radar systems based on boundary scattering transform," *IEICE Trans. Commun.* vol. E87-B, No.5, pp.1357-1365, May, 2004.

[9] M. Helbig, M. A. Hein, U. Schwarz, J. Sachs, "Preliminary investigations of chest surface identification algorithms for breast cancer detection" Proc. IEEE International Conference on Ultra-Wideband, pp. 195-198, 2008.